This is an *Accepted Manuscript*, which has been through the Royal Society of Chemistry peer review process and has been accepted for publication.

Accepted Manuscripts are published online shortly after acceptance, before technical editing, formatting and proof reading. Using this free service, authors can make their results available to the community, in citable form, before we publish the edited article. We will replace this *Accepted Manuscript* with the edited and formatted *Advance Article* as soon as it is available.

You can find more information about *Accepted Manuscripts* in the **Information for Authors**.

Please note that technical editing may introduce minor changes to the text and/or graphics, which may alter content. The journal's standard **Terms & Conditions** and the **Ethical guidelines** still apply. In no event shall the Royal Society of Chemistry be held responsible for any errors or omissions in this *Accepted Manuscript* or any consequences arising from the use of any information it contains.

Journal Name

ChemComm Accepted Manuscript

COMMUNICATION

Solution-processed new porphyrin-based small-molecules as electron donors for highly efficient organic photovoltaics

Song Chen,[a§] Liangang Xiao,[b§] Xunjin Zhu,[a*] Xiaobing Peng,[b*] Wai-Kwok Wong,[a*] and Wai-Yeung Wong[a*]

**A series of unsymmetrical π-conjugated small molecules have been constructed from *meso*-alkyl substituted porphyrins as central unit and 3-ethylrhodanine as terminal group. Using PC$_{71}$BM as acceptor, and these small molecules as electron donors in solution-processed bulk-heterojunction solar cells, a high power conversion efficiency of 6.49% has been achieved.**

Going with the development of accessible and renewable energy sources, solution-processed bulk heterojunction organic solar cells (BHJ OSCs) have been well developed and recognized as one of the most promising next-generation green technology alternatives to inorganic solar cells because of their solution processability, low cost, light weight, and flexibility.[1,2] Specifically, small molecule BHJ OSC have attracted much attention recently, in which small molecule as donor material have defined molecular structure and molecular weight, high purity, and less batch-to-batch variations in comparison with their polymer counterparts.[3-5] With tireless efforts of researchers in the past decade, power conversion efficiencies (PCEs) of solution processed small-molecule based OPVs have been improved up to 10% for single layer bulk hetero-junction (BHJ) solar cells, which are approaching to those of the widely investigated polymer based OPVs.[6-11] And the typical structures of small molecules with high efficiencies in BHJ SM-OSC are mainly dithienosilole-benzo-thiadiazole derivatives[12-15], benzodithiophene (BDT) derivatives[16,17] and oligothiophene derivatives[18], thus searching for new potential donor materials with appropriate physical properties such as low band gap, suitable energy levels, high crystallinity, decent solubility, etc. is critical.[19]

In dye-sensitized solar cells, porphyrin-based push-pull photosensitizers have demonstrated their successes for their large and rigid planar conjugated structures, which can enhance the π-electron delocalization and promote intermolecular π-π interaction, as well as charge transport in devices.[20] However, porphyrin-based either polymers or small molecules (SM) have less contribution in BHJ OSC, and the main performance impediments are the unfavorable aggregation, short exciton diffusion length and the low charge mobility.[21-23] Very recently, Peng et al. employed a porphyrin molecule with less bulky substituents at the periphery as donor material along with PC$_{61}$BM as the acceptor for solution processed organic solar cells and achieved a PCE up to 7.23%.[24] We believe that porphyrin-based small molecules should play a more important role in BHJ OSCs with judicious structural optimization due to their strong absorption spectrum, high molar absorption coefficients, and unique photophysical properties. In the traditional porphyrin structures, peripheral *meso*-phenyl substituents stand almost orthogonal orientation relative to the porphyrin plane, which prevents the intermolecular π-π stacking, as well as intermolecular charge transport.[25] And the porphyrin framework with *meso*-alkyl chains instead of *meso*-phenyl substituents has never been investigated in the construction of small molecules for BHJ OSC applications.[26,27] It was believed that the long alkyl chain could not only improve the solubility of small molecules in most organic solvents, but also control the film morphology and crystallinity, leading to the enhancement of charge transport.[27]
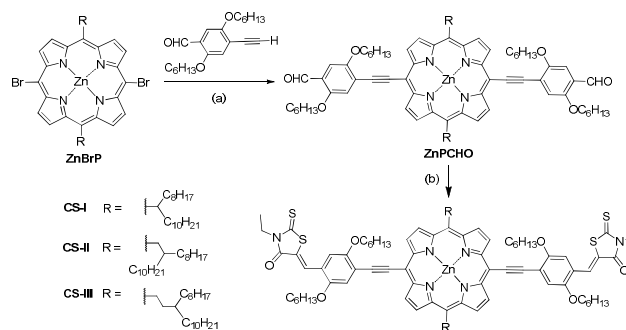
Scheme 1. Synthetic routes for **CS-I**, **CS-II** and **CS-III**. Reaction conditions: a) Pd(PPh$_3$)$_4$, CuI, THF/Et$_3$N, 50°C, overnight; b) 3-ethylrhodanine, dry CHCl$_3$, piperidine, reflux, overnight.

[a.] *Institute of Molecular Functional Materials, Department of Chemistry and Institute of Advanced Materials, Hong Kong Baptist University, Waterloo Road, Kowloon Tong, Hong Kong, P. R. China. Fax: 852 3411 7048; Tel: 852 34115159; E-mail: xjzhu@hkbu.edu.hk; wkwong@hkbu.edu.hk; rwywong@hkbu.edu.hk.*
[b.] *Institute of Polymer Optoelectronic Materials and Devices, State Key Laboratory of Luminescent Materials and Devices, South China University of Technology, 381 Wushan Road, Guangzhou 510640, China. E-mail: chxbpeng@scut.edu.cn*
[§] *S.C. and L.X. contribute equally to this work.*

In this contribution, we first synthesized three new unsymmetrical push-pull A-D-A small molecules consisting of *meso*-alkyl substituted porphyrins 5,15-bis(2-octylundecyl)-porphyrin, 5,15-bis(3-octyl-1-tridecyl)-porphyrin and 5,15-bis(4-octyl-1-tetradecyl)-porphyrin as electron rich donor (D) units, ethynylbenzene as π-linkage, and 3-ethylrhodanine (RH) as electron deficient acceptor (A). Specifically, the effect of the branching point of the alkyl chains on the film morphology, charge mobility and photovoltaic performance was investigated. As shown in **Scheme 1**, the precursors **ZnPCHO** were prepared in about 80% yield via Pd-catalyzed Sonogashira reactions between **ZnBrP** and 4-ethynyl-2,5-bis(hexyloxy)-benzaldehyde. Subsequently, the Knoevengel condensation of **ZnPCHO** with 3-ethylrhodanine afforded the target molecules **CS-I, CS-II and CS-III**. As expected, these three π-conjugated small molecules have good solubility in most common organic solvent.
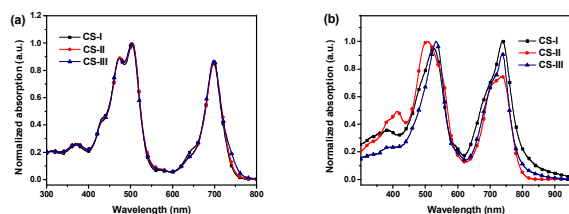

Figure 1. Absorption spectra of **CS-I**, **CS-II** and **CS-III** in CHCl₃ solution (a) and in film (b).

As shown in Fig. 1(a), the UV-Vis absorption spectra of **CS-I**, **CS-II** and **CS-III**, measured in dilute chloroform (CHCl₃) solution exhibits identical peak maxima at around 474, 505 and 698 nm with similar molar extinction coefficients of 1.6×10^5 M^{-1} cm^{-1}. It should be noted that a strong and broad absorption in the region of 600 to 760 nm was observed due the characteristics of A-D-A molecular structure. Compared to their spectra in solution, their thin films prepared by spin-coating from chlorobenzene solutions show about approximately 40 nm red-shifts. Obviously, the strong intermolecular π-π stacking of the molecules leads to a broader absorption from visible to near-infrared (NIR) regions. Such an ordered packing of small molecules is in favor of achieving a efficient charge mobility as discussed below.[28] Besides, **CS-I** in solid film shows a broader absorption band that presumably comes from stronger intermolecular interactions. Compared to **CS-I** and **CS-II**, **CS-III** exhibits blue shift that might be a result of the difference in planarity caused by orientation of the side−chains that stretch out of the porphyrin ring. It is worth noting that **CS-II** in the solid state has a shoulder peak appeared at 414 nm. These phenomena are rather consistent with the difference crystalline nature of **CS-II**. In addition, the optical band gaps of **CS-I**, **CS-II** and **CS-III** in the thin films were estimated from the onset of absorption to be approximately 1.50 eV, 1.55 eV and 1.54 eV, respectively.

Cyclic voltammetry of three small molecules in the solution of CH₂Cl₂ (**Figure S7**, ESI†) was recorded to estimate the highest occupied molecular orbital (HOMO) and lowest unoccupied molecular orbital (LUMO) frontier energy levels. The HOMO and LUMO energy levels were calculated to be −5.12 eV and −3.55 eV (E$_g$ = 1.57 eV) for **CS-I**, −5.14 eV and −3.55 eV (E$_g$ = 1.59 eV) for

CS-II, and −5.17 and −3.54 (E$_g$ = 1.63 eV) for **CS-III**, respectively. Obviously, the presence of the 3-ethylrhodanine in these molecules effectively decreases the bandgaps and extends their absorption into NIR region.[29] On the other hand, the low lying HOMO levels for the three molecules are favorable to generate high open circuit voltage in BHJ OSC and the LUMO levels are higher than PC₇₁BM (−3.8 eV) for exciton dissociation, which indicates the high suitability for them to act as donors and PC₇₁BM as acceptor in BHJ OSCs. As expected, the strategy of combining a weak D and a strong A moiety can provide a favorable HOMO and LUMO energy level, as well as a suitable band gap (E$_g$), which are beneficial for the photovoltaics performance in BHJ OSC.[30]
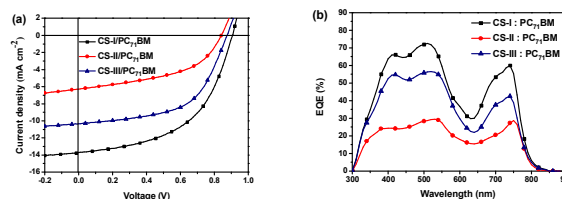

Figure 2. (a) *J-V* curves of the BHJ OSCs based on donor/PC₇₁BM (1:1) under the illumination of AM 1.5G at 100 mW cm^{-2}. (b) EQE curves of the devices based on donor/PC₇₁BM (1:1).

The solution-processed BHJ OSCs were fabricated utilizing PC₇₁BM as the electron acceptor and three small molecules as the electron donors under a conventional device structure of ITO/PEDOT:PSS/donor:PC₇₁BM/poly[(9,9-bis(3'-(N,N-dimethylamino)-propyl)-2,7-fluorene)]-alt-2,7-(9,9-dioctylfluorene PFN)/Al, and then measured under AM 1.5 illumination. The ratio of small molecule donor and PC₇₁BM was optimized to be 1:1 (w/w) and those blend films were processed with or without pyridine additive from chlorobenzene. The current density-voltage (*J-V*) characteristics and external quantum efficiency (EQE) are shown in **Figure 2** and **Figure S8** and **S9** in ESI, and the key device parameters are included in **Table 1**. A PCE of 3.19% with V_{OC} = 0.85 V, J_{SC} = 8.41 mA cm^{-2} and FF = 44.79% was achieved for **CS-I** without pyridine additive (**Figure S8**, ESI†). With 3% pyridine as additive for the blend film, the device shows a much improved photovoltaic performance with V_{OC} = 0.90 V, J_{SC} = 13.72 mA cm^{-2} and FF = 52.12%, corresponding to a PCE of 6.49% (**Figure 2a**). The highly enhanced J_{SC} originates from the change of molecular assembly of the zinc porphyrin in the specific solvent additive.[31] As shown in **Figure 2b**, the external quantum efficiency (EQE) of the optimized device of 1:1 **CS-I**/PC₇₁BM ratio with 3% pyridine and without pyridine additive (**Figure S9**, ESI†) was measured. Both the devices show a very wide range of photocurrent generation in the region of 350 to 800 nm, with the highest EQE value of 72.46% at 510 nm and 60.04% at 740 nm achieved for the device based on blend film with 3% pyridine additive. Unexpectedly, the performance of the device based on **CS-II** shows much inferior performance with a J_{SC} of 6.29 mA cm^{-2}, FF of 0.48 and PCE of 2.53%. This result is due to the inefficient exciton splitting in accordance with the macroscopic phase separation (*vide infra*). As for **CS-III**, a comparable V_{OC} value of 0.87 V and a lower J_{SC} of 10.50 mA cm^{-2} constrain the PCE to 5.12%.

Table 1. Photovoltaic properties of the OSCs based on donor/$PC_{71}BM$ (1:1, with or without additive) under the illumination of AM 1.5 G, 100 mW cm^{-2}.

Donor	J_{SC} (mA cm^{-2})	V_{OC} (V)	FF (%)	PCE (%)	Additive
CS-I	8.41	0.85	44.79	3.19	No
CS-I	13.72	0.90	52.12	6.49	3% pyridine
CS-II	6.29	0.85	47.88	2.53	3% pyridine
CS-III	10.50	0.87	56.87	5.12	3% pyridine

Subsequently, we measured the hole-mobilities of the donor/$PC_{71}BM$ blend films by spin-coating in chlorobenzene with and without pyridine as additive in the space charge limited current (SCLC) method. According to the experimental and calculated results, the hole-mobility of the device without pyridine additive is 1.26×10^{-4} cm^2 V^{-1} s^{-1} for **CS-I**/$PC_{71}BM$ composite film, while the value is highly enhanced to 4.59×10^{-4} cm^2 V^{-1} s^{-1} upon the addition of pyridine (**Figure S10**, ESI†). Obviously, the presence of pyridine in the sample processing plays a very important role in the optimization of photovoltaic efficiency and EQE value, accompanying with the reinforcement of intermolecular interactions and hence an enhanced hole mobility. Noteworthily, **CS-III** demonstrated its space-charge-limited (SCL) hole mobility of 6×10^{-5} cm^2 V^{-1} s^{-1} (**Figure S11**, ESI†), while the films thickness of **CS-II** is not homogeneous and not suitable for the further analysis using SCLC.[32]
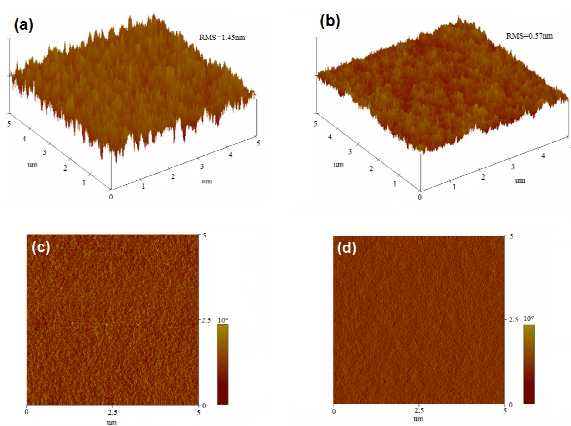
Figure 3. AFM height images (a) and (b) and AFM images (c) and (d) (5 × 5 μm, tapping-mode) of **CS-I**/$PC_{71}BM$ (1:1) composite film prepared without and with 3% pyridine, respectively.

To understand the effect of the molecular structure and the solvent additive on the photovoltaic performance, the morphology of the BHJ thin films spin-coated without and with pyridine additive was characterized by atomic force microscopy (AFM). It was found that the peripheral alkyl substituents could not only enhance the charge mobility of the as-fabricated devices but also affect the morphology of the films.[27] **Figure 3** compares the AFM blend films of **CS-I**/$PC_{71}BM$ thin films cast from chlorobenzene and 3% pyridine in chlorobenzene solutions at the optimized ratio. The blend film without pyridine additive exhibits obvious phase separation between **CS-I** and $PC_{71}BM$ with a root mean square (RMS) roughness of 1.45 nm, which should be unfavorable for exciton diffusion, leading to the lower J_{SC} of the device (**Figure 3a, 3c**).[33] In contrast, a less defined phase separation and smoother surface was found for the **CS-I**/$PC_{71}BM$ blend film in 3% pyridine additive with a root mean square (RMS) roughness of 0.57 nm, due to much better miscibility between **CS-I** and $PC_{71}BM$ in the presence of pyridine (**Figure 3b, 3d**). While the topographic patterns for **CS-II** and **CS-III** appear to possess a rough nodular character when compared to **CS-I**, especially for **CS-II** (**Figure S12**, ESI†). Not surprisingly, the lower surface roughness and much smaller phase separation of the AFM imaging for **CS-I** result in a more efficient exciton dissociation and charge transport, affording higher J_{SC} and higher PCE.

In summary, a series of new unsymmetrical push-pull A-D-A small molecules based on different 5,15-dialkylated porphyrin cores were designed and synthesized, which shows good solubility in common organic solvent, a broad absorption in the visible and NIR regions, a relatively high hole-mobility and good film-forming properties for solution processed BHJ OSC. Based on the blend film of **CS-I**/$PC_{71}BM$ spin-coated from a mixture with 3% pyridine in chlorobenzene, a high PCE of 6.49% was achieved. These primary results indicate that the A-D-A small molecules based on *meso*-alkyl directly substituted porphyrin core are new class of donor candidates for highly efficient BHJ OSC.

Reference

1. G. Li, R. Zhu and Y. Yang, *Nat. Photonics*, 2012, **6**, 153–161.
2. Y. Li, *Accounts Chem. Res.*, 2012, **45**, 723–733.
3. L. M. Chen, Z. Hong, G. Li and Y. Yang, *Adv. Mater.*, 2009, **21**, 1434–1449.
4. J. E. Coughlin, Z. B. Henson, G. C. Welch and G. C. Bazan, *Accounts Chem. Res.*, 2014, 47, 257–270.
5. A. C. Arias, J. D. MacKenzie, I. McCulloch, J. Rivnay and A. Salleo, *Chem. Rev.*, 2010, **110**, 3–24.
6. C. C. Chen, W. H. Chang, K. Yoshimura, K. Ohya, J. You, J. Gao, Z. Hong and Y. Yang, *Adv. Mater.*, 2014, **26**, 5670–5677.
7. J. D. Chen, C. Cui, Y. Q. Li, L. Zhou, Q. D. Ou, C. Li, Y. Li and J. X. Tang, *Adv. Mater.*, 2015, **27**, 1035–1041.
8. H. Kang, S. Kee, K. Yu, J. Lee, G. Kim, J. Kim, J. R. Kim, J. Kong and K. Lee, *Adv. Mater.*, 2015, **27**, 1408–1413.
9. Y. Liu, J. Zhao, Z. Li, C. Mu, W. Ma, H. Hu, K. Jiang, H. Lin, H. Ade and H. Yan, *Nat. Commun.*, 2014, **5**.
10. Q. Zhang, B. Kan, F. Liu, G. Long, X. Wan, X. Chen, Y. Zuo, W. Ni, H. Zhang, M. Li, Z. Hu, F. Huang, Y. Cao, Z. Liang, M. Zhang, T. P. Russell and Y. Chen, *Nat. Photonics*, 2014, **9**, 35–41.
11. B. Kan, Q. Zhang, M. Li, X. Wan, W. Ni, G. Long, Y. Wang, X.

Yang, H. Feng and Y. Chen, *J. Am. Chem. Soc.*, 2014, **136**, 15529–15532.

12. Z. B. Henson, K. Mullen and G. C. Bazan, *Nat. Chem.*, 2012, **4**, 699–704.

13. Y. Sun, G. C. Welch, W. L. Leong, C. J. Takacs, G. C. Bazan and A. J. Heeger, *Nat. Mater.*, 2012, **11**, 44–48.

14. C. J. Takacs, Y. Sun, G. C. Welch, L. A. Perez, X. Liu, W. Wen, G. C. Bazan and A. J. Heeger, *J. Am. Chem. Soc.*, 2012, **134**, 16597–16606.

15. J. A. Love, I. Nagao, Y. Huang, M. Kuik, V. Gupta, C. J. Takacs, J. E. Coughlin, L. Qi, T. S. van der Poll, E. J. Kramer, A. J. Heeger, T. Q. Nguyen and G. C. Bazan, *J. Am. Chem. Soc.*, 2014, **136**, 3597–3606.

16. Y. Lin, L. Ma, Y. Li, Y. Liu, D. Zhu and X. Zhan, *Adv. Energy Mater.*, 2013, **3**, 1166–1170.

17. J. Zhou, Y. Zuo, X. Wan, G. Long, Q. Zhang, W. Ni, Y. Liu, Z. Li, G. He, C. Li, B. Kan, M. Li and Y. Chen, *J. Am. Chem. Soc.*, 2013, **135**, 8484–8487.

18. Y. Chen, X. Wan and G. Long, *Accounts Chem. Res.*, 2013, **46**, 2645–2655.

19. Z. G. Zhang and J. Wang, *J. Mater. Chem.*, 2012, **22**, 4178–4187.

20. E. Dietel, A. Hirsch, E. Eichhorn, A. Rieker, S. Hackbarth and B. Roder, *Chem. Commun.*, 1998, **18**, 1981–1982.

21. J. Hatano, N. Obata, S. Yamaguchi, T. Yasuda and Y. Matsuo, *J. Mater. Chem.*, 2012, **22**, 19258–19263.

22. L. L. Li and E. W. G. Diau, *Chem. Soc. Rev.*, 2013, **42**, 291-304.

23. C. L. Mai, W. K. Huang, H. P. Lu, C. W. Lee, C. L. Chiu, Y. R. Liang, E. W. G. Diau and C. Y. Yeh, *Chem. Commun.*, 2010, **46**, 809–811.

24. H. Qin, L. Li, F. Guo, S. Su, J. Peng, Y. Cao and X. Peng, *Energ. Environ. Sci.*, 2014, **7**, 1397–1401.

25. T. S. Balaban, A. Eichhöfer and J. M. Lehn, *Eur. J. Org. Chem.*, 2000, **2000**, 4047–4057.

26. X. Wang, Y. Wen, H. Luo, G. Yu, X. Li, Y. Liu and H. Wang, *Polymer*, 2012, **53**, 1864–1869.

27. L. Zhou, Z. X. Xu, Y. Zhou, Y. Feng, X. G. Zhou, H. F. Xiang and V. A. L. Roy, *Chem. Commun.*, 2012, **48**, 5139–5141.

28. T. Qin, W. Zajaczkowski, W. Pisula, M. Baumgarten, M. Chen, M. Gao, G. Wilson, C. D. Easton, K. Müllen and S. E. Watkins, *J. Am. Chem. Soc.*, 2014, **136**, 6049–6055.

29. Z. Li, G. He, X. Wan, Y. Liu, J. Zhou, G. Long, Y. Zuo, M. Zhang and Y. Chen, *Adv. Energy Mater.*, 2012, **2**, 74–77.

30. Y. Li, Q. Guo, Z. Li, J. Pei and W. Tian, *Energ. Environ. Sci.*, 2010, **3**, 1427–1436.

31. C. V. Kumar, L. Cabau, E. N. Koukaras, G. D. Sharma and E. Palomares, *Nanoscale*, 2015, **7**, 179–189.

32. J. Zhang, Y. Zhang, J. Fang, K. Lu, Z. Wang, W. Ma and Z. Wei, *J. Am. Chem. Soc.*, 2015, **137**, 8176–8183

33. C. J. Brabec, N. S. Sariciftci and J. C. Hummelen, *Adv. Funct. Mater.*, 2001, **11**, 15–26.